Research Square

Preprints are preliminary reports that have not undergone peer review.
They should not be considered conclusive, used to inform clinical practice,
or referenced by the media as validated information.

Neuropilin-2 is an entry receptor for Chikungunya virus

Yibo Chen
Ke Zhang
Hailin Tang
Zhiwei He
Shudan Luo
Zhongtian Qi
Ping Zhao
Cuiling Ding
cuilingding@smmu.edu.cn

Research Article

Keywords: chikungunya virus, neuropilin-2, receptor, alphavirus, monoclonal antibody

Posted Date: March 12th, 2026

DOI: https://doi.org/10.21203/rs.3.rs-9056403/v1

License: This work is licensed under a Creative Commons Attribution 4.0 International License.
Read Full License

Additional Declarations: The authors declare no competing interests.

Abstract

Chikungunya virus (CHIKV) is a mosquito-borne alphavirus that causes acute febrile illness and chronic arthralgia, yet no approved antivirals exist. Although MXRA8 was previously identified as a CHIKV receptor, it cannot account for viral infection in MXRA8 absence both *in vitro* and *in vivo*, suggesting additional entry mediators. Here, we identify neuropilin-2 (NRP2) as a functional entry receptor for CHIKV. Through targeted siRNA screening in neural cells, we found NRP2 to be critical for viral entry independently of MXRA8. The extracellular domain of NRP2 binds directly to the CHIKV E2 glycoprotein, with defined amino acid residues mediating this interaction. NRP2 and MXRA8 function additively and non-competitively, expanding the known cellular entry landscape for CHIKV. Monoclonal antibodies targeting NRP2 or a soluble NRP2-Fc decoy potently inhibit CHIKV infection *in vitro* and *in vivo*, moreover attenuate joint pathology in a murine model. These findings establish NRP2 as a key entry receptor for CHIKV, explaining its broad tissue tropism and presenting a promising target for therapeutic intervention.

Introduction

Chikungunya virus (CHIKV) is a mosquito-borne alphavirus responsible for over 10 million infections across more than 125 countries or territories in the past two decades[1]. CHIKV causes chikungunya fever (CHIKF), an acute illness characterized by fever, rash, and debilitating arthralgia, with approximately half of patients progressing to chronic rheumatic disease that severely impacts quality of life[2, 3]. Despite its significant burden, no licensed antiviral therapies are currently available[4]. The World Health Organization has classified CHIKV as a priority pathogen requiring urgent attention in the 2024 annual review of disease[5].

The mature CHIKV particle is studded with trimeric spikes composed of E2/E1 heterodimers, which mediate viral entry into host cells[6]. Specifically, the E2 glycoprotein is responsible for binding to receptors on the target cell membrane, whereas E1 drives the low-pH-triggered fusion of the viral envelope with the endosomal membrane following cellular internalization[7, 8]. Extensive research has been conducted to identify cellular receptors for CHIKV[9–13]. Apart from molecules that facilitate viral enrichment at the cell surface, the most significant finding to date is that MXRA8 serves as a functional receptor for CHIKV[9]. Its expression pattern *in vivo* correlates strongly with the development of arthritis upon CHIKV infection[9]. However, several lines of evidence strongly suggest the existence of additional functional receptors for CHIKV[9, 14, 15].Different CHIKV strains exhibit varying dependence on MXRA8[9], and residual infection persists both *in vitro* and *in vivo* in its absence[9, 11, 16].

Accumulating evidence suggests that CHIKV can infect the brain and cause encephalitis[2, 17, 18]. The pathogenic potential of neuroinvasion was underscored by a recent case of severe encephalitis in a recipient of the live-attenuated vaccine Ixchiq[19], which contributed to a subsequent pause in its use by the FDA. Given the characteristically low expression level of the known receptor MXRA8 in the brain[9, 20], we hypothesized that CHIKV utilizes an alternative receptor for neural cell entry. To identify candidate

receptors, we performed a targeted screen of plasma membrane proteins enriched in astrocytes and neurons, primary target cells for CHIKV in the CNS[21, 22], using the Human Protein Atlas (HPA) database[15]. Subsequent functional siRNA screening identified neuropilin-2 (NRP2) as a critical host factor for CHIKV infection.

Here, we establish NRP2 as a functional entry receptor for CHIKV. We demonstrate that NRP2 mediates viral binding and entry independently of MXRA8, directly interacts with the CHIKV E2 glycoprotein, and is required for infection across diverse cell types. Mapping studies define key interacting domains and residues on NRP2. Furthermore, blocking NRP2 with monoclonal antibodies or a soluble NRP2-Fc fusion protein potently inhibits CHIKV infection *in vitro* and ameliorates disease in a murine model. Our findings reveal NRP2 as an entry receptor for CHIKV, explaining its broad tissue tropism and presenting a promising target for therapeutic intervention.

Results

NRP2 promotes CHIKV infection

To identify additional CHIKV entry factors in tissues with low MXRA8 expression, such as the central nervous system (CNS)[20], we screened for plasma membrane proteins highly expressed in human astrocytes and neurons using the HPA database[15]. For astrocytes, we filtered the “protein-class” for “Plasma proteins” and selected the brain expression clusters “19: Astrocytes – mixed function”, “39: Astrocytes – mixed function”, and “40: Astrocytes – neuron interactions”. For neurons, the same plasma protein filter was applied along with clusters associated with neuronal function (Clusters 1, 24, 33, 37, 51, 53, 2, 14, 52). This initial screen yielded 269 astrocyte and 575 neuron membrane-associated molecules (Supplementary Table 1). We excluded proteins localized primarily to intracellular organelles rather than the cell surface. The remaining candidates were further refined based on “Molecular function” using the keywords "receptor" or "host-virus interaction". This resulted in 17 candidate proteins for astrocytes and 15 for neurons (Supplementary Table 2).

The mRNA expression analysis of these 32 molecules, along with MXRA8 across a panel of cell lines (human malignant glioblastoma cell line, U-87 MG; human neuroblastoma cell line, SH-SY5Y; human hepatocellular carcinoma cell line, HuH-7; human bone osteosarcoma epithelial cell line, U-2 OS) recapitulated the *in vivo* expression profile[20, 23] (Supplementary Fig. 1a, b). We then designed siRNAs to knock down each candidate and evaluated their impact on CHIKV infection in SH-SY5Y and U-87 MG cells (Fig. 1a, Supplementary Fig. 1c). CHIKV infection was markedly attenuated by MXRA8 knockdown in SH-SY5Y cells but remained unchanged in U-87 MG cells (Fig. 1b). Given the low abundance of MXRA8 in U-87 MG cells, this differential effect can be explained by the involvement of alternative host factors in mediating viral entry. Knockdown of NRP2 or GP6 proteins significantly attenuated CHIKV infection, regardless of cell type (Fig. 1b). Knockdown of the previously reported replication factor CD81[13], impaired infection only in U-87 MG cells (Fig. 1a, b). TGFBR3, GRIN2C, and NR2C1 affect CHIKV infection

in SH-SY5Y cells, whereas ADGRB1, CNTFR, EGFR, GALR2, and GNB1 showed effects in U-87 MG cells (Fig. 1a).

NRP2 is well known for its role in facilitating axonal guidance during the development of the neuronal system[24]. Given its high expression in multiple CNS cell types[25], especially in astrocytes, and its broad expression in known CHIKV target cells (e.g., fibroblasts, macrophages, endothelial cells) [23], we prioritized it for further investigation as a potential pan-tissue host factor. Using three independent siRNAs, we confirmed that NRP2 knockdown reduced intracellular CHIKV RNA and protein levels (Fig. 1c, d, Supplementary Fig. 1d) and diminished progeny virion release (Fig. 1e, Supplementary Fig. 1e) in SH-SY5Y, U-87 MG, HuH-7, and U-2OS cells. siRNA-1, selected for its superior knockdown efficiency (Fig. 1d), significantly reduced NRP2 surface expression in U-87 MG cells as measured by flow cytometry (Fig. 1f). Conversely, NRP2 overexpression enhanced CHIKV infection in multiple cell types (Fig. 1g). Because NRP2 could not be completely knocked out with RNAi, we successfully generated a NRP2-knockout (KO) monoclonal U87-MG cell line, by using CRISPR-Cas9 (Supplementary Fig. 1f). As respected, compared with wild type (WT) cells, knockout of NRP2 inhibited CHIKV infection (Fig. 1h). The levels of intracellular viral RNA and viral proteins were significantly reduced in the U87-MG KO cells (Fig. i-j). Trans-complementation of NRP2 in U87-MG KO cells restored infectivity (Fig. k-m). And, both knockdown and knockout of NRP2 did not affect cell viability of U87-MG cells (Supplementary Fig. 1g-h). Collectively, these data identify NRP2 as a host factor for CHIKV infection.

a. SH-SY5Y and U-87 MG cells were transfected with siRNAs targeting 32 candidate proteins, with MXRA8-targeting siRNA used as a control, inoculated with CHIKV at an MOI of 1, and processed for immunofluorescence assay. b. Representative immunofluorescence images are shown. c–e. SH-SY5Y, U-87 MG, HuH-7, and U-2 OS cells were transfected with three independent siRNAs targeting NRP2 and inoculated with CHIKV at an MOI of 1. c. Western blot analysis of total lysates using monoclonal antibodies against NRP2 and CHIKV E1. GAPDH served as a loading control. d. CHIKV RNA levels were measured by RT-qPCR. e. Plaque assays were performed to determine viral titers in supernatants. f. U-87 MG cells (par) were tested for NRP2 surface expression by flow cytometry using anti-NRP2 antibody. One representative experiment of two is shown. g. Lysates of infected cells were analyzed by western blot using antibodies against NRP2 and E1 of CHIKV. GAPDH served as a loading control. h-j. Wild-type (WT) or NRP2 knockout (KO) U-87 MG cells were inoculated with CHIKV, and the infection rate (h), CHIKV RNA (i) and protein (j) levels were analyzed. k-m. U-87 MG KO cells overexpressed of NRP2 were inoculated with CHIKV, and protein levels (k), the infection rate (l), and CHIKV RNA levels (m) were analyzed. Data are mean ± SD of 3 independent experiments. Scale bar: 400 μm. *$p < 0.05$, **$p < 0.01$, ***$p < 0.001$, ****$p < 0.0001$. (by Student's t-test or one-way ANOVA).

NRP2 mediates CHIKV cell entry

NRP2 serves as a key receptor for the cellular uptake of a diverse range of ligands via endocytosis[26–28]. Thus, we speculated that NRP2 functions during the viral entry stage. A pseudovirus with CHIKV

structural proteins that can mimic the entry of CHIKV was used to infect WT and KO U-87 MG cells. NRP2 knockout inhibited CHIKV pseudovirus infection (Fig. 2a). To further confirm the effect of NRP2 on CHIKV entry, a NRP2 polyclonal antibody was used to block NRP2 at three different time points: 1 hour before CHIKV inoculation, simultaneously with CHIKV inoculation, and 3 hours after CHIKV inoculation. Blocking NRP2 with antibodies 3 hours after CHIKV inoculation had no inhibitory effect on viral infection (Fig. 2b, Supplementary Fig. 2a-b), pinpointing its role to the early entry phase. Heparan sulfate (HS) is a known CHIKV attachment factor[29]. Enzymatic removal of cell-surface HS reduced infection (25%) but did not abolish the additional inhibitory effect of NRP2 knockdown (Fig. 2c), demonstrating that NRP2 facilitates entry independently of HS.

To better understand the role of NRP2 in viral entry, the effects of NRP2 on viral binding and internalization were evaluated. Both CHIKV binding and internalization in NRP2 knockout and knockdown cells were significantly lower than those in control cells (Fig. 2d, e, Supplementary Fig. 2c). Confocal microscopy confirmed a highly colocalization between NRP2 and CHIKV particles during the binding stage (Fig. 2f), along with fewer bound virions on NRP2-knockout cells (Fig. 2g), which was further corroborated in NRP2-knockdown cells (Supplementary Fig. 2d-e). These results establish NRP2 as an entry factor for CHIKV.

a. A CHIKV-glycoprotein pseudovirus was used to infect WT and KO U-87 MG cells (MOI = 1, 24h). n = 3 independent experiments. b. A NRP2 polyclonal antibody (proteintech 27193-1-AP) was administrated at 10 μg/mL 1 hour before, simultaneously, or 3 hours after CHIKV inoculation (MOI = 1). The infection rate was quantified by enumerating E1-positive cells via fluorescence microscopy. c. WT and NRP2-knockdown U-87 MG cells were treated with bacterial heparinase I, II, and III, inoculated with CHIKV, and analyzed via IF assay. Scale bar: 400 μm.d. Schematic overview of the binding and internalization assay. e. The effect of NRP2 knockout on CHIKV (MOI = 20) binding and internalization in U-87 MG cells via RT-qPCR. f. Co-localization of CHIKV particles (MOI = 10) with the NRP2 protein on the plasma membrane of WT and KO U-87 MG cells was observed by confocal microscopy. NRP2 was stained with a human anti-NRP2-B1 antibody, and CHIKV was stained with a rabbit anti-CHIKV antibody. Scale bar: 10 μm. g. CHIKV virions (MOI = 10) binding to the plasma membrane of WT and KO U-87 MG cells was observed by confocal microscopy. CHIKV was stained with a mouse anti-CHIKV antibody, and the membrane was labeled with a rabbit anti-Na^+/K^+-ATPase antibody. Scale bar: 10 μm. Data are mean ± SD of 3 independent experiments. $^{**}p<0.01$, $^{***}p<0.001$, $^{****}p<0.0001$. (by Student's t-test).

NRP2 binds directly to CHIKV E2

To further analyze the physical interaction between NRP2 and CHIKV, CHIKV E1/E2 heterodimers, E2 proteins, and the NRP2 protein were overexpressed in HEK293T cells. A co-IP assay revealed an interaction between NRP2 and CHIKV E1/E2 heterodimers, specifically with the E2 glycoprotein (Fig. 3a-b). Given the E2 is responsible for the binding of CHIKV to host receptors, we focused on investigating the interaction between NRP2 and E2. A purified recombinant protein comprising the NRP2 extracellular

domain (NRP2-Fc, residues 23–595) bound directly to both recombinant E2 protein and authentic CHIKV virions in ELISA assays (Fig. 3c, Supplementary Fig. 3a). Flow cytometry showed that NRP2-Fc binding to CHIKV-infected cell surfaces was attenuated upon NRP2 knockdown (Fig. 3d). Biolayer interferometry (BLI) further confirmed the NRP2-CHIKV interaction (Supplementary Fig. 3b). Functionally, NRP2-Fc competitively inhibited infection by both authentic CHIKV and CHIKV pseudoviruses, with IC ~ 50 ~ values of 1.773 μg/mL and 2.975 μg/mL, respectively (Fig. 3e, f, Supplementary Fig. 3c).

To identify the domain(s) of NRP2 responsible for E2 binding, expression constructs containing different domains of NRP2 were generated, guided by the atomic structure[30] (Fig. 3g). Pulldown and co-IP assays indicated that E2 binds to regions containing the A2, B1, and B2 domains of NRP2 (Fig. 3h, Supplementary Fig. 3d-i). We then introduced full-length and truncated NRP2 to refractory HCT116 cells and infected them with CHIKV for 24h, after which the intracellular viral RNA and the protein levels were measured. Only full-length NRP2, and not individual domain truncations, could rescue CHIKV infection when expressed in HCT116 cells (Fig. 3i, Supplementary Fig. 3j-m), indicating that an intact extracellular structure is required for functional receptor activity.

Further to identify the key amino acid sites of NRP2 mediating cell entry of CHIKV, structural prediction of the NRP2–CHIKV E2 complex was performed using AlphaFold 3 (AF3). The resulting model implicates four specific amino acid residues (D199, K209, E197, D252) on NRP2 as being pivotal for mediating binding to the CHIKV E2 protein (Fig. 3j). Then, we generated a panel of 5 mutants of NRP2. 4 single mutations (D199K, K209D, E197K, D252K) and their combinations (199-252K/D) were introduced into NRP2. We next overexpressed these NRP2 mutants in HCT116 cells. 24 hours later, these cells were then infected with CHIKV-NAY and the efficiency of infection was analyzed using WB, IF, RT-qPCR and plaque experiments as described above (Fig. 3k-m, Supplementary Fig. 3n-o). As demonstrated in Fig. 3k, 3l and 3m, mutations at position D199, K209, E197 and D252 all reduced NRP2-mediated virus infection. The D199K substitution had the most significant impact, reducing the infection of CHIKV nearly as much as did the combination of all 4 substitutions in the NRP2.

a-b. HEK293T cells were co-transfected with plasmids encoding flag-tagged NRP2 and his-tagged E1/E2 (a) or E2 (b) for 48 h. Cell lysates were subjected to immunoprecipitation (IP) using anti-flag or anti-his antibodies, followed by immunoblotting (IB) with rabbit anti-NRP2 (proteintech 27193-1-AP), mouse anti-his (proteintech 66005-1-Ig), or anti-CHIKV E2 (Mybiosource MBS1568592) antibodies. c. ELISA analysis of the binding between NRP2 and E2 (Left) or CHIKV virions (Right). d. Binding of NRP2-Fc to WT and NRP2-knockdown U-87 MG cells infected with CHIKV. Cells were infected with CHIKV for 9.5 h and processed for NRP2-Fc binding by flow cytometry using an Alexa Fluor 488-conjugated goat anti-human IgG secondary antibody. e-f. Competitive inhibition of CHIKV infection by NRP2-Fc. SH-SY5Y cells were treated with NRP2-Fc and inoculated with authentic CHIKV (e) or CHIKV pseudovirions (f). g. Schematic diagram of the design of all NRP2 truncation plasmids. h. His-tagged E2 protein was immobilized on beads and incubated with lysates from HEK293T cells overexpressing vector control, flag-tagged full-length NRP2, or the NRP2 truncations described in (g). Bound proteins were analyzed by immunoblotting with rabbit anti-flag (Abclonal AE092) antibody. i. HCT116 cells overexpressing vector control, flag-

tagged NRP2, or the NRP2 truncations were infected with CHIKV. Protein levels were analyzed by western blotting using anti-flag, anti-CHIKV E1, and anti-GAPDH (loading control) antibodies. j. The structure of the NRP2-CHIKV E2 complex was predicted using AlphaFold 3 (AF3). Residues involved in CHIKV E2 are labeled in blue, and those in NRP2 are labeled in red. k-m. HCT116 cells were transfected with either a vector control, flag-tagged NRP2, or flag-tagged NRP2 carrying the mutated key amino acids and inoculated with CHIKV. Protein levels (k), the infection rate (l), and viral RNA (m) were analyzed. Scale bar: 400 μm. ****p<0.0001. (by one-way ANOVA).

NRP2 and MXRA8 function independently

MXRA8 has been identified as a functional receptor for CHIKV[7, 9]. We next investigated the relationship between NRP2 and the established receptor MXRA8 during CHIKV entry. Overexpression of either NRP2 or MXRA8 in refractory HCT116 cells enhanced CHIKV susceptibility (MXRA8 (574.1%) or NRP2(773.4%)), and co-expression had an additive effect (3337.2%) (Fig. 4a, b, Supplementary Fig. 4a). Zhang et al. [9] reported different CHIKV strains show variable dependence on MXRA8, we tested the dependence of 5 different CHIKV strains (181/25, AF15561, ROSS, LR2006, NAY) on NRP2 and MXRA8. All tested strains were dependent on NRP2, with LR2006 and NAY showing particularly strong reliance (Fig. 4c). While, ROSS, LR2006 and NAY showed less dependence on MXRA8, compared with 181/25 and AF15561. Similarly, simultaneous knockdown of both molecules produced a more pronounced reduction (80.2%) in infection than single knockdowns (MXRA8 (41%) or NRP2 (68%)) (Fig. 4d, Supplementary Fig. 4b). To further validate this, we blocked MXRA8 and NRP2 either individually or in combination with polyclonal antibodies at 1 hour before CHIKV inoculation (Fig. 4e, Supplementary Fig. 4c). Combined antibody blockade of NRP2 and MXRA8 yielded superior inhibitory efficacy (85.5%) compared to individual blockade in both infection (MXRA8 (54%) or NRP2(66.5%)) (Fig. 4e) and viral binding assays (Fig. 4f). Structural analysis indicated that the reported MXRA8 binding site on E2[7] and the predicted NRP2 binding site are distinct and non-overlapping (Fig. 4g). Consistent with this, competitive ELISA demonstrated no mutual interference between MXRA8 and NRP2 for binding to E2 (Fig. 4h). These results demonstrate that NRP2 and MXRA8 function as independent, non-competing entry receptors for CHIKV.

a-b. HCT116 cells were transfected to overexpress NRP2, MXRA8, or both (NRP2 + MXRA8), followed by CHIKV infection. Viral infection (a) and protein levels (b) were analyzed by IF or western blotting using anti-NRP2, anti-MXRA8, and anti-CHIKV E1 antibodies. GAPDH was used as a loading control. c. SH-SY5Y cells were transfected to knockdown NRP2 or MXRA8 and inoculated with different CHIKV strains. Viral infection was assessed by IF using siNC as a control. d. SH-SY5Y cells were transfected with siNRP2, siMXRA8, or both (siNRP2 and siMXRA8), inoculated with CHIKV and processed to IF assay. e-f. SH-SY5Y cells were treated with anti-NRP2, anti-MXRA8 antibodies, or both (NRP2 Ab and MXRA8 Ab) 1 h before infection with CHIKV. The infection rate (e) and the level of bound viral RNA (f) were measured by IF or RT-qPCR. g. Alignment of the binding sites between CHIKV E2 and MXRA8 or NRP2. Residues involved in CHIKV E2 binding to MXRA8 are labeled in red, and those for CHIKV E2 binding to NRP2 are

labeled in blue. h. Competitive ELISA analysis of the binding between NRP2 and E2 (Left) or CHIKV virions (Right) pre-incubated with MXRA8-Fc. Data are mean ± SD of 3 independent experiments. Scale bar: 400 μm. *p<0.05, **p<0.01, ***p<0.001, ****p<0.0001. (by one-way ANOVA).

Targeting NRP2 inhibits CHIKV infection

To begin to assess the physiological importance of NRP2 interaction with CHIKV, we evaluated the anti-CHIKV effect of two high-affinity, fully humanized monoclonal antibodies (mAbs) targeting the human NRP2 A2 (A2 Ab) and B1 (B1 Ab) domains [31] on SH-SY5Y and U-87 MG cells in a dose-dependent manner, with IC50 values in the sub-μg/mL range. No inhibition was observed when antibodies were added post-entry (Supplementary Fig. 5a). Due to high sequence conservation (Supplementary Fig. 5b-c), these mAbs targeting human NRP2 also inhibited CHIKV infection in mouse MEF and NIH/3T3 cells as expected (Supplementary Fig. 4d).

We next assessed therapeutic efficacy in a C57BL/6 mouse model of CHIKV-induced arthritis. Mice received a single intravenous dose of NRP2-Fc, A2 Ab, B1 Ab, or a non-binding control antibody (NB Ab) immediately prior to footpad inoculation with CHIKV (Fig. 5c). No significant changes in bodyweight between the treatment and control groups (Fig. 5d). All treatments significantly ameliorated footpad swelling compared to the control group, with peak efficacy at 6 days post-infection (dpi) (Fig. 5e-f). Moreover, treatments substantially reduced viral loads in ipsilateral and contralateral ankle joints and calf muscles at 3 dpi (Fig. 5g). Histopathological analysis of footpads at 6 dpi revealed that NRP2-Fc and the mAbs markedly attenuated CHIKV-induced inflammation and tissue damage (Fig. 5h-i). These findings underscore the critical role of NRP2 in CHIKV pathogenesis and demonstrate the *in vivo* therapeutic potential of NRP2 blockade.

Figure 5. Targeting NRP2 blocks CHIKV infection both in vitro and in vivo

a-b. SH-SY5Y and U-87 MG cells were treated with A2 Ab or B1 Ab 1 hour before CHIKV infection with (MOI = 1). (Lower panels) Virus-positive cells were quantified by IF, and the infection rate data points were fitted using nonlinear regression to calculate the IC50. (Upper panels) Cell viability was assessed using CCK-8 reagent to calculate the CC50. c. Schematic of the therapeutic regimen for the CHIKV-induced arthritis mouse model treated with NRP2-Fc, A2 Ab or B1 Ab. d-i. NRP2-Fc, A2 Ab or B1 Ab (200 μg per mouse) were administered via tail vein injection prior to subcutaneous inoculation of 10^2 PFU CHIKV in the left hind foot. d-e. Daily monitoring of mouse body weight change (d) and footpad swelling (e) in the NB Ab control group, treatment groups, and mock-infected controls. f. Statistical analysis of footpad thickness on 6 dpi, the peak of disease manifestation. g. Absolute quantification of viral RNA levels by RT-qPCR in the ipsilateral or contralateral ankle joints and calf muscles of mice from each group on 3 dpi. h. Histopathological scoring of footpads from each group on 6 dpi. i. Representative H&E-stained images of footpads from each group on 6 dpi. Data are mean ± SD of 3 independent experiments. **p<0.01, ****p<0.0001. (by one-way ANOVA).

Discussion

The broad cell and tissue tropism of CHIKV has long suggested the involvement of multiple entry receptors[29]. Here, we identify NRP2 as a functional entry receptor for CHIKV, operating independently of the known receptor MXRA8. This dual-receptor model explains the virus's ability to infect a wide range of tissues, including the MXRA8-low CNS, and accounts for the residual, MXRA8-independent infection observed previously.

Our targeted screen in neural cells identified several potential host factors, with NRP2 emerging as the most impactful. We systematically validated its role: NRP2 is required for viral binding and entry across diverse cell types; its extracellular domain binds directly to the CHIKV E2 glycoprotein; it functions additively and without competition with MXRA8; and its blockade by mAbs or soluble decoys potently inhibits infection *in vitro* and *in vivo*.

NRP2, a single-pass transmembrane glycoprotein, is well-established as a co-receptor for class 3 semaphorins[24, 26] and vascular endothelial growth factors (VEGFs)[27, 28], playing critical roles in axonal guidance, angiogenesis, and immune regulation[32–34]. Recent studies have implicated NRP2 as a host factor for other viruses, including Lujo virus [30, 35] and human cytomegalovirus [36–38], indicating an evolutionarily conserved role in pathogen engagement. Interestingly, different viruses engage distinct NRP2 domains: Lujo virus uses the A1 domain[35], while HCMV and, as we show here, CHIKV utilize the A2 domain[37]. This highlights NRP2's versatility as a viral receptor. Furthermore, we found that NRP2 knockdown also inhibits infection of related alphaviruses, Sindbis virus and Ross River virus, but not several flaviviruses (Supplementary Fig. 6), suggesting it may serve as a common receptor for multiple alphaviruses.

Despite these findings, there are certain limitations in our study. The use of primary human cells, cerebral organoids, and NRP2 knockout mice would further solidify its role in CHIKV neuroinvasion and systemic infection. Additionally, while we show NRP2 and MXRA8 act independently, their interplay with other reported host factors like TIM-1, AXL, or prohibitin[12, 29, 39, 40] in different cellular contexts warrants future investigation.

In conclusion, we expand the paradigm of CHIKV cellular entry by identifying NRP2 as a key receptor. The compelling *in vivo* efficacy of NRP2-targeting agents underscores its high therapeutic potential. Given the lack of approved antivirals for CHIKV, targeting NRP2 represents a promising strategy for developing broad-spectrum countermeasures against CHIKV and potentially other alphaviruses.

Methods

Mice, cells and viruses

Wild-type C57BL/6J mice of matched sex and age were obtained from Shanghai Cyper-BK Experimental Animal Co. Animals were maintained in individually ventilated cages (up to eight mice per cage) with free access to food and water. Housing conditions consisted of a 12-hour light/dark cycle, ambient temperature of 24°C, and relative humidity of 40–60%.

The SH-SY5Y (CRL-2266; ATCC), HuH-7 (SCSP-526, Chinese Academy of Sciences, Shanghai, China), HEK-293T (CRL-3216; ATCC), U-2 OS (HTB-96; ATCC), C2C12 (CRL-1772; ATCC), NIH/3T3 (CRL-1658; ATCC) and U-87 MG (HTB-14; ATCC) cell lines were maintained in Dulbecco's Modified Eagle Medium containing 10% fetal bovine serum (FBS) and 1% penicillin-streptomycin. All cells were cultured at 37°C with 5% CO_2.

The CHIKV-NAY strain (MN402883.1) was isolated from a laboratory-confirmed CHIKF patient. CHIKV-181/25, AF15561, ROSS, LR2006 were all obtained through reverse genetics construction. All experiments involving live CHIKV were performed in a Biosafety Level 3 (BLS-3) laboratory of the Navy Medical University. The experimental protocols were reviewed and approved by the Institutional Animal Care and Use Committee of the university.

Plasmid construction

The NRP2 overexpressing plasmid was constructed by inserting the cDNA of NRP2 (NM_201266.2) into the mammalian expression vector pCMV3 with a Flag tag at the C-terminus. The overexpressing plasmid E1E2 was constructed by inserting the cDNA of CHIKV E1 and CHIKV E2 into pCDNA3.1(+) with a His tag at the C-terminus. The overexpressing plasmid E2 was constructed by inserting the cDNA of CHIKV E2 into pCDNA3.1(+) with a His tag at the C-terminus. The NRP2 mutant was constructed by the individual or combined deletion of four specific segments: A1, A2, B1, and B2. The NRP2 amino acid mutant was constructed by introducing mutations to disrupt four specific amino acid residues at positions 199, 197, 209 and 252 using the QuickChange Site-Directed Mutagenesis kit. The overexpressing plasmid MXRA8 was constructed by inserting the cDNA of MXRA8 into pCDNA3.1(+) with a His tag at the C-terminus.

siRNA and Plasmid Transfection

Transfections were performed in 96- or 24-well plates. For the 96-well plates, 10 μL of Opti-MEM containing 0.4 μL of Lipofectamine 2000 was mixed with 10 μL of Opti-MEM containing either 0.4 μL of siRNA (20 μM) or 160 ng of plasmid. The mixture was incubated at room temperature for 15 min and then added to SH-SY5Y or U-87 MG cells, followed by supplementation with 80 μL of Opti-MEM. For the 24-well plates, 50 μL of Opti-MEM containing 2 μL of Lipofectamine 2000 was mixed with 50 μL of Opti-MEM containing either 2 μL of siRNA (20 μM) or 800 ng of plasmid. The siRNA-transfected SH-SY5Y or U-87 MG cells were maintained at 37°C for 48 h before they were infected with CHIKV.

Immunofluorescence (IF)

Cells infected with CHIKV, RRV, SINV, TBEV, YFV, WNV, JEV, or ZIKV were fixed with 4% paraformaldehyde for 20 minutes at room temperature. Permeabilization was performed using 0.1% Triton X-100 for 10 minutes, followed by blocking with 3% bovine serum albumin for 2 hours. The cells were then incubated

overnight at 4℃ with the following primary antibodies: anti-CHIKV E1 pAb, anti-RRV E1 pAb, anti-SINV E1 pAb, anti-TBEV NS1 mAb, anti-YFV NS1 pAb, anti-WNV NS1 pAb, anti-JEV NS1 pAb, or anti-ZIKV NS1 pAb. Subsequently, staining was performed using appropriate Alexa Fluor™ 488-conjugated secondary antibodies. Nuclei were counterstained with DAPI. Images were acquired using a BioTek Lionheart FX imaging reader. The percentage of infected cells (infectivity) was calculated and normalized to the control group.

RT-qPCR

To quantify the mRNA levels of target genes or CHIKV RNA in cells under various treatments, the total RNA was first extracted. Subsequently, cDNA was synthesized by reverse transcription using the PrimeScript™ RT Master Mix kit (Takara). The cDNA was then analyzed by quantitative real-time PCR using the TB Green Premix Ex Taq™ kit (Takara) on an Applied Biosystems QuantStudio™ 3 system. The relative expression levels of the target genes were calculated using the $2^{-\Delta\Delta Ct}$ method, with GAPDH serving as the internal reference control. The sequences of the specific primers used are listed in Supplementary Table 3.

Cell viability assay

Cell viability was determined using a Cell Counting Kit-8 (CCK-8) according to the manufacturer's instructions. Briefly, SH-SY5Y, U-87 MG, HuH-7, or U-2 OS cells were seeded in 96-well plates and transfected with siNRP2 for 48 hours (with siNC serving as the control). The culture medium was then replaced with 100 µL of fresh medium containing 10 µL of CCK-8 solution per well. Following incubation at 37°C for 1.5 h, the absorbance at 450 nm was measured using a microplate reader (Biotek).

Surface staining of NRP2

U-87 MG cells were collected with trypsin and washed twice with pre-cold wash buffer consisting of Hank's Balanced Salt Solution (HBSS) supplemented with 15 mM HEPES and 2% fetal bovine serum (FBS). Cells were then incubated with an anti-NRP2 (human) monoclonal antibody (1 mg/mL, diluted 1:400) at 4°C for 30 min. After washing twice, cells were stained with an AF488-conjugated goat anti-human secondary antibody at 4°C for 30 min in the dark. After two additional washes, the cells were resuspended in PBS and analyzed by flow cytometry.

Western Blot Analysis

After three washes with PBS, the treated cells were harvested using a RIPA lysis buffer supplemented with protease inhibitors. The cell lysates were centrifuged at 10,000 × g for 5 min. The resulting supernatants were mixed with SDS loading buffer (final concentration 1×) and boiled for 10 min. The samples were loaded onto a 12.5% polyacrylamide gel, and proteins were separated by electrophoresis at a constant voltage of 80 V. Subsequently, the separated protein bands were transferred onto a PVDF membrane. The membrane was blocked with 5% skim milk (prepared in TBST containing 0.1% Tween-20) at room temperature for 2 h. After blocking, the membrane was then incubated with the corresponding primary antibody at 4°C overnight. Following three washes with TBST, the membrane was incubated with

the appropriate HRP-conjugated secondary antibody for 2 h at room temperature. After washing three times with TBST, the target protein bands were visualized using a supersignal Western blot detection reagent and a chemiluminescence imaging system (Clinx). The band intensities were quantified using Image J software (version 1.54g).

Plaque Assay

Vero cells were seeded in 24-well plates and cultured to 100% confluency. After washing twice, serially diluted virus (10-fold steps in 2% DMEM) was added and allowed binding for 2 h at 37°C, with gentle rocking every 15 min. After removal of the inoculum and two PBS washes, cells were overlaid with 1 mL/well of carboxymethylcellulose medium (1.5% CMC, 2% FBS, 1% GlutaMAX, 1% penicillin-streptomycin, 1% non-essential amino acids). Plaques were counted after fixed and stained with crystal violet.

Removal of cell-surface glycosaminoglycans

To remove glycosaminoglycans, including heparan sulfate, from the cell surface, U-87 MG or SH-SY5Y cells were treated with a mixture of bacterial heparinases I, II, and III (purchased from New England Biolabs). An enzyme cocktail was prepared by combining 1 µL each of heparinase I, II, and III with 97 µL of reaction buffer (20 mM HEPES [pH 7.5], 150 mM NaCl, 4 mM $CaCl_2$, 0.1% BSA). Cells were incubated with the enzyme mixture at 37°C for 1 h. Following three washes with culture medium, cells were incubated with CHIKV at 37°C for 2 h. The inoculum was then removed, replaced with 2% DMEM maintenance medium, and cells were cultured for an additional 22 h at 37°C. Subsequently, cells were fixed with methanol. CHIKV infection was evaluated by IF assay, and positively infected cells were quantified.

Pseudotyped virus experiments

CHIKV pseudotyped virus was generated by co-transfecting HEK-293T cells with plasmids encoding the HIV-1 structural proteins (gag-pol) and the structural proteins of CHIKV (strain LR2006). The pseudovirus self-assembled and packaged a luciferase reporter gene. Pseudovirus entry in normal or NRP2-knockdown U-87 MG cells was assessed by measuring luciferase activity using a Luciferase Reporter Gene Assay Kit 48 h later.

Generation and production of NRP2-Fc, A2 monoclonal antibody and B1 monoclonal antibody

A cDNA fragment encoding the human NRP2 extracellular domain(residues 23–595, GenBankaccession NM_201266.2)and the human IgG2a-Fcwere synthesized, and inserted into pCDNA3.4vector.Following sequence verification, the NRP2-Fc construct was expressed in CHO cells. One day prior to transfection, cells were seeded at 0.3 × 10^6 cells/mL. For transfection, cells were harvested by centrifugation, then resuspended in electroporation buffer containing the plasmid DNA, and subjected to electrical pulse. Pre-warmed culture medium was added immediately post-transfection. Transfected cells were supplemented with culture medium 24 h later. The culture supernatant was collected four days post-

transfection, clarified by centrifugation at 3,000 × g for 15 minutes, and the target protein was purified using Protein A affinity chromatography columns. The eluted protein was dialyzed into a buffer containing 120 mM NaAc-HAc and 70 mM arginine (pH 5.5), filtered through a 0.22μm filter, and stored at -80°C. The purity of the NRP2-Fc protein was assessed by SDS-PAGE and SEC-HPLC, and endotoxin levels were determined. The sequences of A2-Ab and B1-Ab antibodies were from the reference[31]. These two monoclonal antibodies were also produced using the same CHO expression system.

Antibody blocking assay

The polyclonal antibody against NRP2 (Proteintech, Cat No. 27193-1-AP), and two monoclonal antibodies against NRP2-A2 or NRP2-B1 were used for the antibody blocking assay. For pre-treatment, SH-SY5Y cells were placed on ice for 15 min, followed by a 1 h incubation on ice with 50 μL of serially diluted monoclonal antibodies. Then 50 μL of purified virus (MOI = 3) was added per well, and cells were incubated at 37°C for 2 h. In concurrent treatment, cells were incubated with a mixture of antibody and virus for 2 h at 37°C. For post-treatment, cells were first infected with virus for 3 h, then diluted antibodies were added and incubated for another 2 h. After infection, the medium in all groups was replaced with 2% DMEM maintenance medium. Cells were fixed 24h after infection and analyzed by IF assay to determine infection rates.

Blocking assays with NRP2-Fc

For the NRP2-Fc blocking assay, serially diluted NRP2-Fc or a negative control (NB-Ab) was incubated with the virus at an MOI of 3 in a total volume of 100 μL for 1 h at 37°C. The mixture was then added to SH-SY5Y or U-87 MG cells and incubated for 24 h. Subsequently, the cells were fixed, and the infection rates were measured by IF assay.

Viral binding assay

For the viral binding assay, the antibody-treated or siRNA-transfected SH-SY5Y or U-87 MG cells in 24-well plates were infected with CHIKV (MOI 20) at 4°C for 2 h. The cells were then washed three times with cold PBS and collected for viral RNA extraction and detection by RT-qPCR.

Viral internalization assay

For the viral internalization assay, the siRNA-transfected SH-SY5Y or U-87 MG cells in 24-well plates were infected with CHIKV (MOI 20) at 4°C for 2 h. The cells were washed 3 times with cold PBS and maintained at 37°C for 2 h. Then, the cells were washed 3 times with cold PBS and treated with proteinase K at 4°C for 0.5 h to remove the virus retained on the surface of the plasma membrane. After that, the cells were collected for viral RNA extraction and quantified via RT-qPCR.

Co-immunoprecipitation(Co-IP) Assay

For the Co-IP assay, cells from different co-transfection groups were lysed. The supernatants of the cell lysates were incubated with either an anti-Flag antibody or an anti-His antibody on a flip shaker at 4°C for

12 h (control groups received an equivalent amount of isotype-matched IgG antibody). Subsequently, 20 µl of Protein G Agarose beads were added to each sample, followed by incubation for 3 h at 4°C with gentle agitation on a flip shaker. After conjugation, the Protein G Agarose beads were collected by centrifugation and washed four times. The beads were then resuspended in 1× SDS loading buffer and boiled for 5 min. The eluted proteins were finally analyzed by western blot analysis.

Pull-down Assay

For the pull-down assay, concentrated and purified recombinant E2E1-His or E2-His protein expressed in eukaryotic cells was used. HEK293T cells overexpressing the target protein (Flag-tag) were lysed, and the supernatants of the cell lysates were co-incubated with the E2E1-His or E2-His protein on a flip shaker at 4°C for 12 h. Subsequently, an anti-Flag antibody or an anti-His antibody was added, followed by incubation on a flip shaker at 4°C for 8 h. Subsequently, 20 µl of Protein G Agarose beads were added to each sample, followed by incubation for 3 h at 4°C with gentle agitation on a flip shaker. After conjugation, the Protein G Agarose beads were collected by centrifugation and washed four times. The beads were then resuspended in 1× SDS loading buffer and boiled for 5 min. The eluted proteins were finally analyzed by western blot analysis.

Expression of CHIKV VLPs

CHIKV virus-like particles (VLPs) were produced by transfecting HEK-293F cells with a plasmid encoding the structural proteins of CHIKV (strain NAY). The culture supernatant was collected 48 hours post-transfection, concentrated 100-fold, and filtered through a 0.22µm filter. VLPs were then purified by discontinuous sucrose density gradient centrifugation and dialyzed against PBS.

Bio-layer interferometry (BLI) -based NRP2 binding assay

Binding interactions between NRP2 and CHIKV VLPs were analyzed using BLI on an Octet RED384 instrument (Sartorius). Recombinant NRP2-Fc was immobilized at 5 µg/mL on His1K biosensors. CHIKV VLPs were diluted 10-fold in running buffer (PBS, pH 7.4, supplemented with 0.1% BSA and 0.1% Tween-20) and associated with the biosensor for 120 seconds, followed by a 180-second dissociation step. Binding sensograms were processed and analyzed using the Octet Data Analysis 12.0 software.

ELISA-based NRP2-Fc binding assays

Anti-CHIKV E2 mouse monoclonal antibody was coated onto ELISA plates at 4 µg per well in sodium bicarbonate buffer (pH 9.3) and incubated overnight at 4°C. Plates were washed 4 times with PBST (containing 0.1% Tween-20) and blocked with 3% BSA in PBST at 37°C for 1 h. CHIKV-NAY was diluted to 2×10^7 PFU/mL in 2% BSA, added at 100 µL per well, and incubated for 1 h at room temperature. After four washes, serially diluted NRP2-Fc or a corresponding negative control (non-binding antibody, NB Ab) was added and incubated for 1 h at room temperature. Following another wash, plates were incubated with horseradish peroxidase (HRP)-conjugated goat anti-human IgG (H + L) (1:2000 dilution) for 2 h at room temperature. After a final wash with PBST, the reaction was developed using 3,3',5,5'-

tetramethylbenzidine substrate and stopped with 2 M H_2SO_4. Absorbance at 450 nm was measured using a microplate reader. To assess direct protein interaction, ELISA plates were coated with 4 μg E2 protein per well. After blocking, serially diluted NRP2-Fc was added directly to the wells. The remaining steps were performed as described above.

Cell-based NRP2-Fc binding assay

U-87 MG cells were first transfected with siNRP2 for 48 hours and then inoculated with CHIKV (MOI of 3, 10h), followed by detachment using trypsin and collection. After two washes with cold buffer (HBSS supplemented with 15 mM HEPES and 2% FBS), the cells were incubated with 1 μg/mL NRP2-Fc at 4°C for 30 min. After washing twice with the cold buffer, cells were stained with an AF488-conjugated anti-human secondary antibody at 4°C for 30 minutes in the dark. Following two additional washes, the cells were resuspended in PBS and analyzed by flow cytometry.

Mouse experiments

NRP2-Fc, A2 Ab, B1 Ab, or NB Ab (control) (200 μg per mouse in PBS) was administered to six-week-old male C57BL/6 mice via tail vein injection. Concurrently, all mice were inoculated subcutaneously in the footpad with 100 PFU of CHIKV-NAY or PBS (mock). Footpad swelling was monitored daily for 10 days via left foot measurements (width x height) using digital calipers. At 3 days post-infection (dpi), mice were euthanized. After washing with PBS, the ipsilateral (left) and contralateral (right) ankle joints and calf muscles were harvested, and viral loads were quantified by RT-qPCR. At the peak of swelling (day 6), mice were euthanized and the left footpads were fixed for hematoxylin and eosin (H&E) staining and histopathological analysis.

Statistical analysis

GraphPad Prism 10 for Windows was used to generate figures and for statistical analysis (GraphPad Software). Cell culture experiments were analyzed by unpaired t-test, or ANOVA with a multiple comparison correction depending on data distribution and the number of comparison groups. Analysis of levels of joint swelling or viral burden *in vivo* was determined by one-way ANOVA.

Declarations

Author contributions

Y.B.C. validated the siRNA library in cells. Y.B.C. performed infectivity studies with authentic viruses. Y.B.C. and C.L.D. designed and executed immunoprecipitation, ELISA and BLI experiments. Y.B.C. and Z.W.H. performed virus attachment and internalization experiments, including analysis of confocal microscopy data. Y.B.C. performed *in vivo* challenge studies with assistance from H.L.T., S.D.L. and Z.W.H. C.L.D., P.Z., Z.T.Q. and K.Z. provided project supervision and participated in study conceptualization. C.L.D., P.Z. and Z.T.Q. acquired funding. C.L.D., Y.B.C. and P.Z. wrote the original draft of the manuscript and all of the authors participated in reviewing and editing.

Competing interests

The authors declare no competing interests

* **Correspondence:** Cuiling Ding, Ping Zhao, Zhongtian Qi, Department of Microbiology, Faculty of Naval Medicine, Naval Medical University, 800 Xiangyin Rd, Shanghai, 200433, China. E-mail address: cuilingding@smmu.edu.cn, ORCID: 0000-0001-7899-1586; pnzhao@163.com, ORCID: 0000-0002-1289-326X; qizt@smmu.edu.cn, ORCID: 0000-0003-4163-0853.

References

1. Suhrbier, A. Rheumatic manifestations of chikungunya: emerging concepts and interventions. *Nature reviews. Rheumatology* **15**, 597-611 (2019).
2. de Souza, W.M. *et al.* Pathophysiology of chikungunya virus infection associated with fatal outcomes. *Cell host & microbe* **32**, 606-622.e608 (2024).
3. Kang, H. *et al.* Chikungunya seroprevalence, force of infection, and prevalence of chronic disability after infection in endemic and epidemic settings: a systematic review, meta-analysis, and modelling study. *The Lancet. Infectious diseases* **24**, 488-503 (2024).
4. Wang, M., Wang, L., Leng, P., Guo, J. & Zhou, H. Drugs targeting structural and nonstructural proteins of the chikungunya virus: A review. *International journal of biological macromolecules* **262**, 129949 (2024).
5. Organization., W.H. Pathogens prioritization: A scientific framework for epidemic and pandemic research preparedness.2024-07-30. https://www.who.int/publications/m/item/pathogens-prioritization-a-scientific-framework-for-epidemic-and-pandemic-research-preparedness. (2025).
6. Kril, V., Aïqui-Reboul-Paviet, O., Briant, L. & Amara, A. New Insights into Chikungunya Virus Infection and Pathogenesis. *Annual review of virology* **8**, 327-347 (2021).
7. Song, H. *et al.* Molecular Basis of Arthritogenic Alphavirus Receptor MXRA8 Binding to Chikungunya Virus Envelope Protein. *Cell* **177**, 1714-1724.e1712 (2019).
8. Voss, J.E. *et al.* Glycoprotein organization of Chikungunya virus particles revealed by X-ray crystallography. *Nature* **468**, 709-712 (2010).
9. Zhang, R. *et al.* Mxra8 is a receptor for multiple arthritogenic alphaviruses. *Nature* **557**, 570-574 (2018).
10. Kirui, J. *et al.* The Phosphatidylserine Receptor TIM-1 Enhances Authentic Chikungunya Virus Cell Entry. *Cells* **10** (2021).
11. Reyes Ballista, J.M. *et al.* Chikungunya virus entry and infectivity is primarily facilitated through cell line dependent attachment factors in mammalian and mosquito cells. *Frontiers in cell and developmental biology* **11**, 1085913 (2023).
12. Wintachai, P. *et al.* Identification of prohibitin as a Chikungunya virus receptor protein. *Journal of medical virology* **84**, 1757-1770 (2012).

13. Lasswitz, L. *et al.* The Tetraspanin CD81 Is a Host Factor for Chikungunya Virus Replication. *mBio* **13**, e0073122 (2022).
14. atlas, T.h.p. (2025).
15. Das, T. *et al.* Chikungunya fever: CNS infection and pathologies of a re-emerging arbovirus. *Progress in neurobiology* **91**, 121-129 (2010).
16. Basore, K. *et al.* Cryo-EM Structure of Chikungunya Virus in Complex with the Mxra8 Receptor. *Cell* **177**, 1725-1737.e1716 (2019).
17. Gérardin, P. *et al.* Chikungunya virus-associated encephalitis: A cohort study on La Réunion Island, 2005-2009. *Neurology* **86**, 94-102 (2016).
18. Nyamwaya, D.K. *et al.* Incidence of chikungunya virus infections among Kenyan children with neurological disease, 2014-2018: A cohort study. *PLoS medicine* **19**, e1003994 (2022).
19. Mosnier, E. *et al.* Fatal Adverse Event After VLA1553 Chikungunya Vaccination in an Elderly Patient: A Case Report From Reunion Island. *Open forum infectious diseases* **12**, ofaf550 (2025).
20. Atlas, T.H.P. (2025).
21. Wei Chiam, C., Fun Chan, Y., Chai Ong, K., Thong Wong, K. & Sam, I.C. Neurovirulence comparison of chikungunya virus isolates of the Asian and East/Central/South African genotypes from Malaysia. *The Journal of general virology* **96**, 3243-3254 (2015).
22. Eleftheriadou, I. *et al.* Selective transduction of astrocytic and neuronal CNS subpopulations by lentiviral vectors pseudotyped with Chikungunya virus envelope. *Biomaterials* **123**, 1-14 (2017).
23. atlas, T.h.p. (2025).
24. Chen, H., Chédotal, A., He, Z., Goodman, C.S. & Tessier-Lavigne, M. Neuropilin-2, a novel member of the neuropilin family, is a high affinity receptor for the semaphorins Sema E and Sema IV but not Sema III. *Neuron* **19**, 547-559 (1997).
25. Tran, T.S. *et al.* Secreted semaphorins control spine distribution and morphogenesis in the postnatal CNS. *Nature* **462**, 1065-1069 (2009).
26. Suzuki, K., Kumanogoh, A. & Kikutani, H. Semaphorins and their receptors in immune cell interactions. *Nature immunology* **9**, 17-23 (2008).
27. Kärpänen, T. *et al.* Functional interaction of VEGF-C and VEGF-D with neuropilin receptors. *FASEB journal : official publication of the Federation of American Societies for Experimental Biology* **20**, 1462-1472 (2006).
28. Gluzman-Poltorak, Z., Cohen, T., Herzog, Y. & Neufeld, G. Neuropilin-2 is a receptor for the vascular endothelial growth factor (VEGF) forms VEGF-145 and VEGF-165 [corrected]. *The Journal of biological chemistry* **275**, 18040-18045 (2000).
29. McAllister, N. *et al.* Chikungunya Virus Strains from Each Genetic Clade Bind Sulfated Glycosaminoglycans as Attachment Factors. *Journal of virology* **94** (2020).
30. Raaben, M. *et al.* NRP2 and CD63 Are Host Factors for Lujo Virus Cell Entry. *Cell host & microbe* **22**, 688-696.e685 (2017).

31. Xu, Z. *et al.* Inhibition of VEGF binding to neuropilin-2 enhances chemosensitivity and inhibits metastasis in triple-negative breast cancer. *Science translational medicine* **15**, eadf1128 (2023).
32. Yuan, L. *et al.* Abnormal lymphatic vessel development in neuropilin 2 mutant mice. *Development (Cambridge, England)* **129**, 4797-4806 (2002).
33. Roy, S. *et al.* Multifaceted Role of Neuropilins in the Immune System: Potential Targets for Immunotherapy. *Frontiers in immunology* **8**, 1228 (2017).
34. Roy, S. *et al.* Macrophage-Derived Neuropilin-2 Exhibits Novel Tumor-Promoting Functions. *Cancer research* **78**, 5600-5617 (2018).
35. Cohen-Dvashi, H., Kilimnik, I. & Diskin, R. Structural basis for receptor recognition by Lujo virus. *Nature microbiology* **3**, 1153-1160 (2018).
36. Martinez-Martin, N. *et al.* An Unbiased Screen for Human Cytomegalovirus Identifies Neuropilin-2 as a Central Viral Receptor. *Cell* **174**, 1158-1171.e1119 (2018).
37. Kschonsak, M. *et al.* Structural basis for HCMV Pentamer receptor recognition and antibody neutralization. *Science advances* **8**, eabm2536 (2022).
38. Wrapp, D. *et al.* Structural basis for HCMV Pentamer recognition by neuropilin 2 and neutralizing antibodies. *Science advances* **8**, eabm2546 (2022).
39. Gardner, C.L. *et al.* Deliberate attenuation of chikungunya virus by adaptation to heparan sulfate-dependent infectivity: a model for rational arboviral vaccine design. *PLoS neglected tropical diseases* **8**, e2719 (2014).
40. Jemielity, S. *et al.* TIM-family proteins promote infection of multiple enveloped viruses through virion-associated phosphatidylserine. *PLoS pathogens* **9**, e1003232 (2013).

Figures

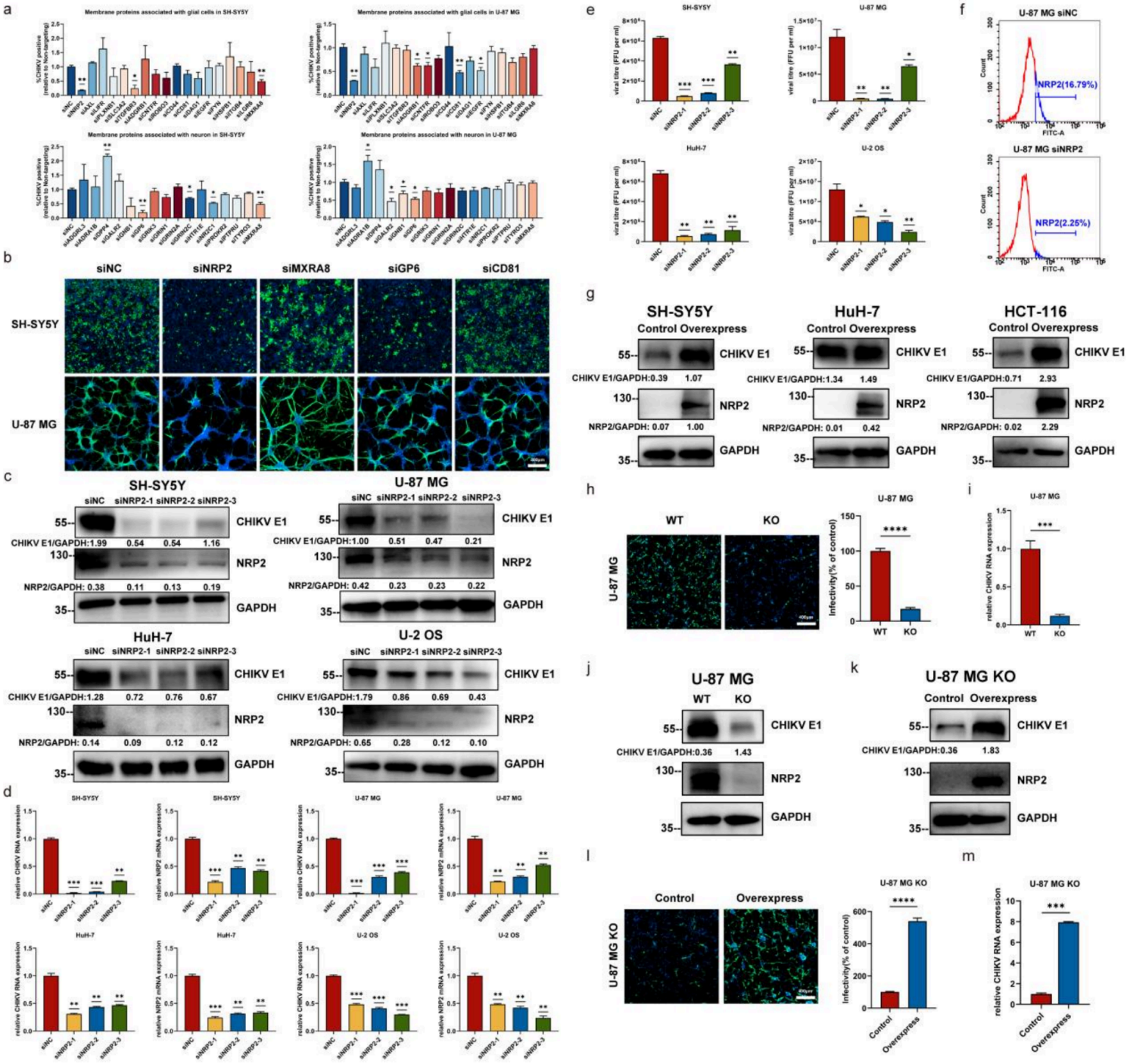


Figure 1

NRP2 is a critical host factor for CHIKV infection.

a. SH-SY5Y and U-87 MG cells were transfected with siRNAs targeting 32 candidate proteins, with MXRA8-targeting siRNA used as a control, inoculatedwith CHIKV at an MOI of 1, and processed for immunofluorescence assay. b. Representative immunofluorescence images are shown. c–e. SH-SY5Y, U-87 MG, HuH-7, and U-2 OS cells were transfected with three independent siRNAs targeting NRP2 and inoculated with CHIKV at an MOI of 1. c. Western blot analysis of total lysates using monoclonal antibodies against NRP2 and CHIKV E1. GAPDH served as a loading control. d. CHIKV RNA levels were

measured by RT-qPCR.e. Plaque assays were performed to determine viral titers in supernatants. f. U-87 MG cells (par) were tested for NRP2 surface expression by flow cytometry using anti-NRP2 antibody. One representative experiment of two is shown. g. Lysates of infected cells were analyzed by western blot using antibodies against NRP2 and E1 of CHIKV. GAPDH served as a loading control. h-j. Wild-type (WT) or NRP2 knockout (KO) U-87 MG cellswere inoculated with CHIKV, and the infection rate (h), CHIKV RNA (i) and protein (j) levels were analyzed. k-m. U-87 MG KO cells overexpressed of NRP2 were inoculated with CHIKV, and protein levels (k), the infection rate (l), and CHIKV RNA levels (m) were analyzed. Data are mean ± SD of 3 independent experiments. Scale bar: 400 μm. *p < 0.05, **p < 0.01, ***p < 0.001, ****p < 0.0001. (by Student's t-test or one-way ANOVA).

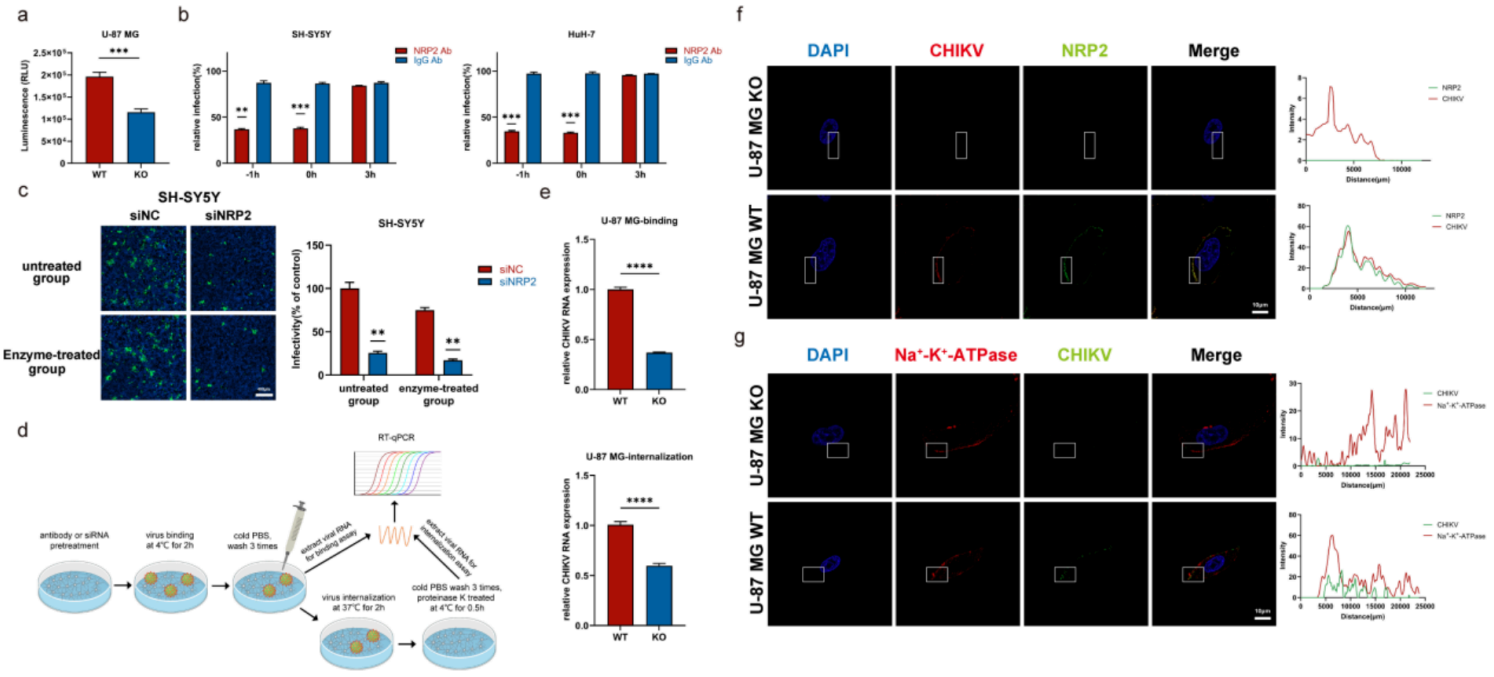


Figure 2

NRP2 acts as an entry factor for CHIKV.

a. A CHIKV-glycoprotein pseudovirus was used to infect WT and KO U-87 MG cells (MOI=1, 24h). n=3 independent experiments. b. A NRP2 polyclonal antibody (proteintech 27193-1-AP) was administrated at 10 μg/mL 1 hour before, simultaneously, or 3 hours after CHIKV inoculation (MOI=1). The infection rate was quantified by enumerating E1-positive cells via fluorescence microscopy. c. WT and NRP2-knockdown U-87 MG cells were treated with bacterial heparinase I, II, and III, inoculated with CHIKV, and analyzed via IF assay. Scale bar: 400 μm.d. Schematic overview of the binding and internalization assay. e. The effect of NRP2 knockout on CHIKV (MOI=20) binding and internalization in U-87 MG cells via RT-qPCR. f. Co-localization of CHIKV particles (MOI=10) with the NRP2 protein on the plasma membrane of WT and KO U-87 MG cells was observed by confocal microscopy. NRP2 was stained with a human anti-NRP2-B1 antibody, and CHIKV was stained with a rabbit anti-CHIKV antibody. Scale bar: 10 μm. g. CHIKV virions (MOI=10) binding to the plasma membrane of WT and KO U-87 MG cells was observed by confocal microscopy. CHIKV was stained with a mouse anti-CHIKV antibody, and the membrane was

labeled with a rabbit anti-Na^+/K^+-ATPase antibody. Scale bar: 10 μm. Data are mean ± SD of 3 independent experiments. **p□0.01, ***p□0.001, ****p□0.0001. (by Student's t-test).

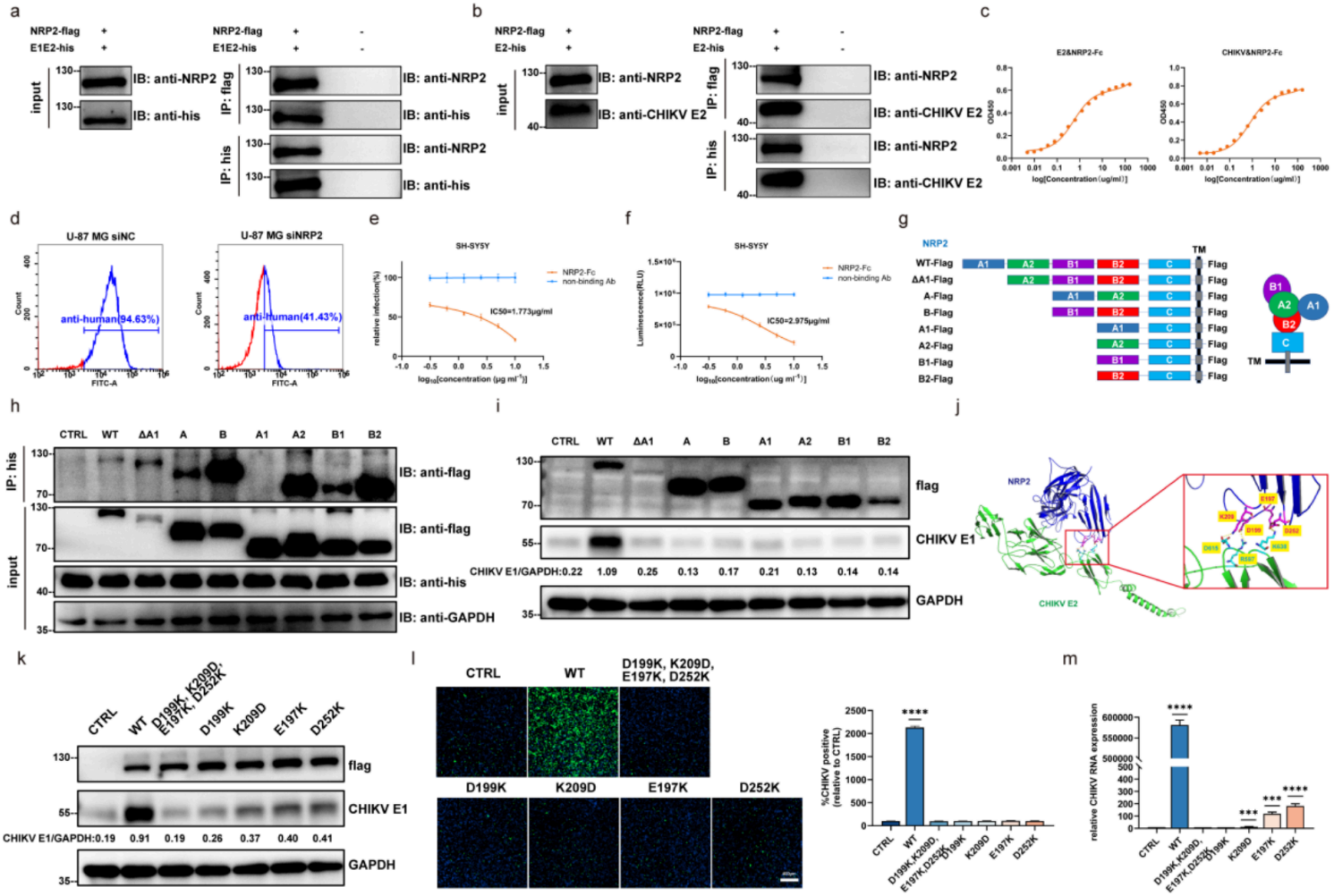


Figure 3

NRP2 binds to the CHIKV E2.

a-b. HEK293T cells were co-transfected with plasmids encoding flag-tagged NRP2 and his-tagged E1/E2 (a) or E2 (b) for 48 h. Cell lysates were subjected to immunoprecipitation (IP) using anti-flag or anti-his antibodies, followed by immunoblotting (IB) with rabbit anti-NRP2 (proteintech 27193-1-AP), mouse anti-his (proteintech 66005-1-Ig), or anti-CHIKV E2 (Mybiosource MBS1568592) antibodies. c. ELISA analysis of the binding between NRP2 and E2 (Left) or CHIKV virions (Right). d. Binding of NRP2-Fc to WT and NRP2-knockdown U-87 MG cells infected with CHIKV. Cells were infected with CHIKV for 9.5 h and processed for NRP2-Fc binding by flow cytometry using an Alexa Fluor 488-conjugated goat anti-human IgG secondary antibody. e-f. Competitive inhibition of CHIKV infection by NRP2-Fc. SH-SY5Y cells were treated with NRP2-Fc and inoculated with authentic CHIKV (e) or CHIKV pseudovirions (f). g. Schematic diagram of the design of all NRP2 truncation plasmids. h. His-tagged E2 protein was immobilized on beads and incubated with lysates from HEK293T cells overexpressing vector control, flag-tagged full-length NRP2, or the NRP2 truncations described in (g). Bound proteins were analyzed by immunoblotting with rabbit anti-flag (Abclonal AE092) antibody. i. HCT116 cells overexpressing vector control, flag-

tagged NRP2, or the NRP2 truncations were infected with CHIKV. Protein levels were analyzed by western blotting using anti-flag, anti-CHIKV E1, and anti-GAPDH (loading control) antibodies. j. The structure of the NRP2-CHIKV E2 complex was predicted using AlphaFold 3 (AF3). Residues involved in CHIKV E2 are labeled in blue, and those in NRP2 are labeled in red. k-m. HCT116 cells were transfected with either a vector control, flag-tagged NRP2, or flag-tagged NRP2 carrying the mutated key amino acids and inoculated with CHIKV. Protein levels (k), the infection rate (l), and viral RNA (m) were analyzed. Scale bar: 400 μm. ****p<0.0001. (by one-way ANOVA).

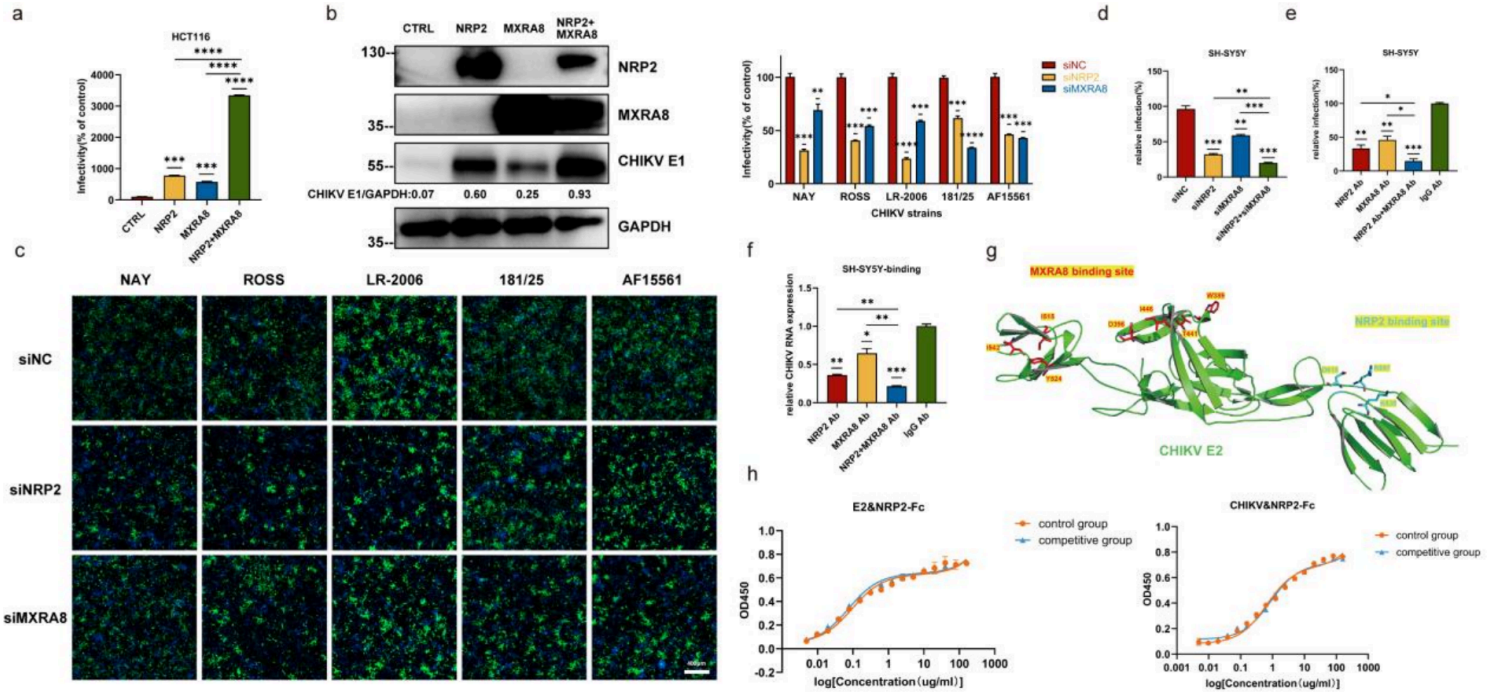


Figure 4

NRP2 and MXRA8 function independently in mediating CHIKV entry

a-b. HCT116 cells were transfected to overexpress NRP2, MXRA8, or both (NRP2+MXRA8), followed by CHIKV infection. Viral infection (a) and protein levels (b) were analyzed by IF or western blotting using anti-NRP2, anti-MXRA8, and anti-CHIKV E1 antibodies. GAPDH was used as a loading control. c. SH-SY5Y cells were transfected to knockdown NRP2 or MXRA8 and inoculated with different CHIKV strains. Viral infection was assessed by IF using siNC as a control. d. SH-SY5Y cells were transfected with siNRP2, siMXRA8, or both (siNRP2 and siMXRA8), inoculated with CHIKV and processed to IF assay. e-f. SH-SY5Y cells were treated with anti-NRP2, anti-MXRA8 antibodies, or both (NRP2 Ab and MXRA8 Ab) 1 h before infection with CHIKV. The infection rate (e) and the level of bound viral RNA (f) were measured by IF or RT-qPCR. g. Alignment of the binding sites between CHIKV E2 and MXRA8 or NRP2. Residues involved in CHIKV E2 binding to MXRA8 are labeled in red, and those for CHIKV E2 binding to NRP2 are labeled in blue. h. Competitive ELISA analysis of the binding between NRP2 and E2 (Left) or CHIKV virions (Right) pre-incubated with MXRA8-Fc. Data are mean ± SD of 3 independent experiments. Scale bar: 400 μm. *p<0.05, **p<0.01, ***p<0.001, ****p<0.0001. (by one-way ANOVA).

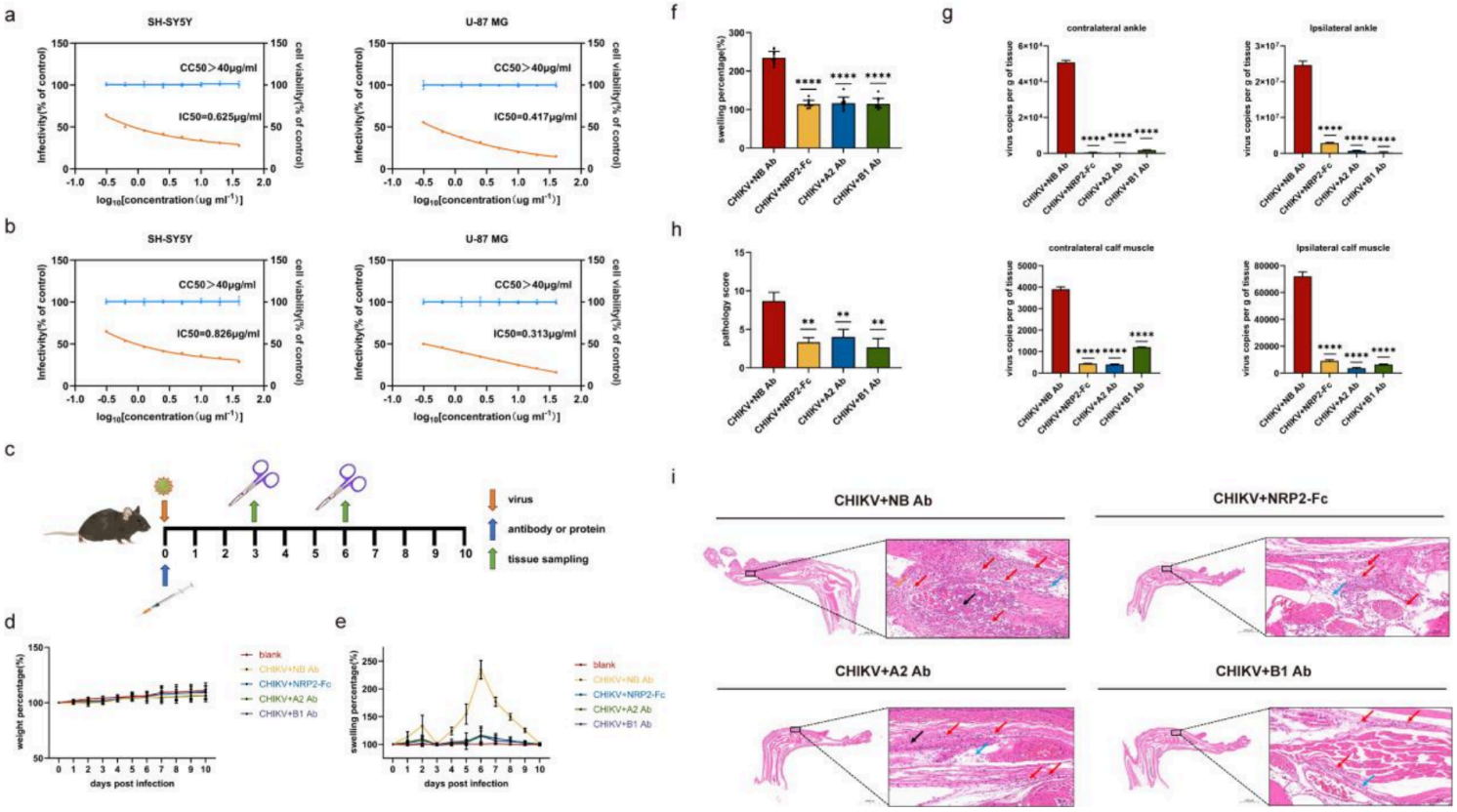


Figure 5

Targeting NRP2 blocks CHIKV infection both in vitro and in vivo

a-b. SH-SY5Y and U-87 MG cells were treated with A2 Ab or B1 Ab 1 hour before CHIKV infection with (MOI=1). (Lower panels) Virus-positive cells were quantified by IF, and the infection rate data points were fitted using nonlinear regression to calculate the IC50. (Upper panels) Cell viability was assessed using CCK-8 reagent to calculate the CC50. c. Schematic of the therapeutic regimen for the CHIKV-induced arthritis mouse model treated with NRP2-Fc, A2 Ab or B1 Ab. d-i. NRP2-Fc, A2 Ab or B1 Ab (200 μg per mouse) were administered via tail vein injection prior to subcutaneous inoculation of 10^2 PFU CHIKV in the left hind foot. d-e. Daily monitoring of mouse body weight change (d) and footpad swelling (e) in the NB Ab control group, treatment groups, and mock-infected controls. f. Statistical analysis of footpad thickness on 6 dpi, the peak of disease manifestation. g. Absolute quantification of viral RNA levels by RT-qPCR in the ipsilateral or contralateral ankle joints and calf muscles of mice from each group on 3 dpi. h. Histopathological scoring of footpads from each group on 6 dpi. i. Representative H&E-stained images of footpads from each group on 6 dpi. Data are mean ± SD of 3 independent experiments. $^{**}p$ 0.01, $^{****}p$0.0001. (by one-way ANOVA).

Supplementary Files

This is a list of supplementary files associated with this preprint. Click to download.

- Supplementaryfigure.docx